Case Study of UAS Videography for Depth Inversion within a Shallow Water Surf Zone along the Texas Gulf Coast

Larissa Marques Freguete[a], Michael J. Starek[a,b], Jacob Berryhill[a,b]
[a]Texas A & M University-Corpus Christi, 6300 Ocean Drive, Corpus Christi, TX USA 78412;
[b] Conrad Blucher Institute of Surveying and Science, Texas A&M University-Corpus Christi, 6300 Ocean Drive, Corpus Christi, TX USA 78412

Abstract

Coastal zones are at the interface of land and sea and provide a buffer to storms, wave action, and coastal inundation. Bathymetric mapping of the submerged littoral zone is essential for the understanding of sediment transport and good coastal management and planning. Surf zones are dynamic areas, ever-changing, so there is a need for low-cost, rapid response aerial remote sensing techniques that can provide high temporal and spatial coverage of nearshore bathymetry. However, this is a challenging task given water turbidity, wave action, seafoam, and other issues. With this motivation, this study used a small unoccupied aircraft system (UAS) equipped with a digital RGB camera to collect video footage of wave action on the water surface. The video data was then used to apply a spectral depth inversion algorithm called cBathy and estimate nearshore bathymetry at high resolution. Ground truth data were collected using cross-shore transect surveys to a depth of 2 m for assessment of the UAS-based bathymetry estimates. The video data was split into frames with a frequency of 2 frames per second (fps), and ground control points (GCPs) laid out in the scene were used to perform image georectification. A time stack of image pixel values was then generated from the video data for the cBathy depth inversion algorithm. Accuracy assessment resulted in an overall RMSE of 0.2056 m for an area of 390 m offshore and 400 m alongshore, and the maximum depth achieved was up to 3 m. Results show the potential of the cBathy algorithm to provide reasonable depth accuracies in dynamic and turbid water surf zones. However, results also show that this method has constraints for which users need to be aware of prior to applying it, including the study site's physical characteristics.

Keywords: cBathy, UAS, bathymetry, videography, coastal zone, ocean waves, surf zone, remote sensing.

1. INTRODUCTION

Coastal zones represent a small portion of the total inhabited area in the world, yet it contains about 40% of the world population which generates strong demand for coastal resources [1,2,3]. Anthropogenic intervention can change the coastal hydrodynamics and affect the sediment budget, which creates the need for understanding well the sediment transport, and having a solid bathymetric record is crucial for it. However, coastal areas are a challenging domain to be mapped due to the action of waves and currents, so that the use of sensors faces the problem of local sediment accretion or erosion which can lead to scouring or burial of bottom-mounted sensors type. The dynamic processes in this area have a very small temporal scale, which means that water level or sediment volume changes can happen in a matter of hours.

Traditionally, ocean floor data is collected by echo sounders installed on vessels, such as single beam echo sounder (SBES) or multibeam echo sounder (MBES). However, such methods have coverage limitations in shallow water surf zones and navigation restrictions. Airborne bathymetric light detection and ranging (LiDAR) is a remote sensing (RS) technique that enables shallow-water bathymetric mapping when water conditions permit, but its effectiveness is severly limited by high water turbidity. It is also a costly approach and only applicable to regional scale mapping due to reliance on traditional piloted aircraft. Over the past decade, there has been an increasing demand for new RS techniques for bathymetric mapping that can provide higher temporal and spatial coverage with lower operational cost and better efficiency as well as the ability to overcome the challenges posed by poor water clarity conditions [4,5].

Due to the flexibility of unoccupied airact system (UAS) paltforms as a remote sensing modality, UAS-based photo-bathymetry techniques provide opportunities to address the above mentioned requirements. According to [6], there are mainly three types of approaches for UAS-based imaging for bathymetric mapping techniques: Structure-from-Motion

Remote Sensing of the Ocean, Sea Ice, Coastal Waters, and Large Water Regions 2021,
edited by Charles R. Bostater, Xavier Neyt, Proc. of SPIE Vol. 11857, 1185702
 · doi: 10.1117/12.2599447

(SfM) photogrammetry, spectral depth inversion, and physics-based modeling approaches to invert depths based on wave properties measued with videography. The latter approach is presently the only method able to provide depth estimation in turbid water conditions. The physics-based modeling approach, also called linear depth inversion, uses the ocean surface features generated by the waves and relates them to an analytical solution. The strategy of this method is to find the wave celerity and derive the water depth by applying the linear wave dispersion relation or a variant [7,8], Eq. 1.

$$c = \sqrt{gh} \qquad \text{Eq. 1}$$

The first study applying the linear depth inversion technique is dated from the 1940s with the work of [9]; however, this technique has been greatly improved since then. The cBathy algorithm is currently one of the more advanced and accurate techniques for applying this approach [10,11]. The cBathy algorithm was developed to overcome the issues faced by the spectral correlation method in areas where the bottom cannot be visualized due to the turbidity or bubbles in the surf zone. So instead of using information from the ocean bottom, the algorithm aims at the surface signatures for estimating the water depth.

This algorithm uses video footage of waves, and it is composed of 3 processing blocks [10]:

1) Frequency-dependent analysis: in this phase, Fourier Transform and empirical orthogonal functions (EOF)-based filtering are used for deriving the four dominant wave frequencies and wavenumbers. Then the depth is estimated for each frequency-wavenumber set.
2) Frequency-independent depth estimation: a single depth value is assigned for each point along with the estimation error.
3) Running-average depth estimation: due to the problem of low-spatial coherence from signals of wave breaking areas, a Kalman filter is used to provide smoothed depth estimates.

The purpose of this study is to consider the applicability of UAS videography for inverting bathymetry within the surf zone, where turbidity is a major limiting factor. Therefore, this study applies and evaluates the performance and applicability of small UAS videography using the cBathy depth inversion algorithm to estimate high resolution bathymetry within a shallow water surf zone.

The following sections will cover the description of the dataset used, main steps for the video pre-processing phase and bathymetry calculation, discussion about the obtained results, and concluding remarks.

2. STUDY AREA AND DATASETS

The study site is a stretch of wave-dominated sandy beach located along Mustang Island, which is a barrier island located along the southern Texas Gulf coastline, USA (Figure 1). Wave characteristics in the region are typically short-period and lower energy wind-driven waves. The open beach site was chosen because it provides a region where the wave linear dispersion can be assumed and so the depth inversion algorithm can be applied.

The UAS video recording was conducted on August 20, 2020, with a cloud-free sky condition, with a forecasted significant wave height of 0.33 m, primary swells of 3 s for the nearshore wave at Fish Pass jetties [12]. The observed waves presented periods ranging between 2-8 s and the measured, and wind gauges reading showed south winds speed up to 11 mph.

The video recording was performed with a DJI Phantom 4 RTK UAS at 70 m above the ground in hovering mode, with a tilt camera angle of 60º off-nadir orientated against the wavefront. At 70 m altitude above ground/water surface level, this resulted in an average ground sample distance (GSD) of approximately 2 cm/pixel. The camera sensor was a 1" CMOS sensor, with an 8.8 m focus length, aperture of f/2.8. The video was recorded in a 4k (3840×2160) resolution, with a frame rate of 30 fps, and with an 11 min and 8s footage duration.

5 ground control points (GCP) consisting of 0.9 m x 0.9 m aerial survey targets were placed in the scene along the exposed beach for image georectification. Ground truthing of bathymetry consisted of collecting 11 cross-shore transects spaced 30 m apart alongshore with cross-shore sample resolution of 1-4 m according to the seafloor homogeneity. Ground truthing for bathymetry values occurred on the day before the flight, and it was performed using a Leica TS06

plus total station with prism pole out to a depth of approximately 2 m. The GCPs were surveyed using real-time kinematic (RTK) GNSS with corrections acquired from the Texas Department of Transportation (TxDOT) real-time network. Horizontal coordinates were recorded in the NAD83 State Plane South Texas coordinate reference system with vertical coordinates (z) referenced to the NAVD88 vertical datum.

Figure 1. Study area and UAS hovering location (red dot).

3. METHODS

Generation of the bathymetry map from the UAS recorded video data was achieved using the cBathy and Quantitative Coastal Imaging MATLAB toolboxes provided by the Coastal Imaging Research Network (CIRN) group (available at https://github.com/Coastal-Imaging-Research-Network). The CIRN toolbox deals with all the procedures of splitting the video into individual images, rectifying the images, and generating the grid for storing the image pixel values in time stacks. On the other hand, the cBathy toolbox deals with the computation of depth by using Fourier analysis, empirical orthogonal functions, and a Kalman filter for estimating the waves physical characteristics (wavelength, frequency, and celerity) and, conversely, the application of the wave dispersion equation for depth estimation. In this section, the explanation of the whole workflow will have a general approach; however, all the steps made followed the methodology presented in [13,14].

3.1 Video data processing

The CIRN toolbox provides functions for splitting the recorded video into oblique images and for performing the frames georectification to build the required data structure for the implementation of the cBathy script. The entire length of the original video footage (~11 minutes) was split into frames with a rate of 2 fps, which generated a total of 1,310 images. Camera calibration was also necessary for defining the video camera's intrinsic orientation (IO) parameters needed for reducing image distortion inherent in the video imagery, which is enhanced on the edges from the oblique perspective. The IO parameters were obtained with MATLAB's Camera Calibration Toolbox. Inside the CIRN toolbox workflow, the camera IO and the GCP's world coordinates and image coordinates, provided by the user manually, are combined for solving the extrinsic orientation (EO) of the camera at the time of each frame.

For solving the EO parameters for each camera frame, static objects (generally GCPs) were selected as reference for tracking the variation of camera pose and for image stabilization. Then, the EO for all camera frames is solved and their rectification is done in a local or world coordinate with limits arbitrarily defined. The local coordinate system was used to avoid large numbers, which can affect the algorithm calculation capacity. The local coordinate grid limits were arbitrarily set, with an extension of 1000 m on the x-axis, and 1050 m on the y-axis. The rectified images were oriented in such a way that the shore trend was aligned with the cartesian y-axis.

3.2 Bathymetric map

A grid region of interest (ROI) for depth calculation was defined with a dimension of 390 m alongshore and 400 m cross-shore, cell resolution of 2 m for both dimensions. The grid ROI was set to cover all the captured area of the shore and avoid long extensions towards the offshore. Every georectified image frame had its pixel intensity values extracted from the grid points. The data structure required by cBathy algorithm is a matrix with a time series of the extracted pixel values with their corresponding coordinates information, which is referred to as pixel instrument. The pixel instrument is the final output from the CIRN toolbox and the primary input for cBathy algorithm.

The cBathy algorithm was then executed with the following settings:

- Analysis domain had the same dimension defined for the pixels instrument grid.
- No tide correction was applied to the depth calculation during the execution of the algorithm.
- The minimum depth limit was left at 0.25 m.
- The range of frequency to be retrieved for the Fourier analysis was set between 1/10 - 1/2 Hz, respecting the period of waves encountered at the site during the study period. The frequency sampling resolution was set to 0.0299 Hz for allowing the calculation of at least 20 wave frequency.
- The number of wave frequencies to be kept for analysis was set to 4. A low number of frequencies was chosen to avoid noise from less frequent waves and higher computation demand.

Because the cBathy method provides results water depth measurements (not seafloor elevations relative to a vertical datum), the accuracy assessment in this work had to conver those values into elevation values relative to the same vertical datum as the ground truth data. Hence, the measured average tide level at the time of flight was subtracted from the depth values for setting it into a local vertical datum and then a conversion to NAVD88 vertical daum was achieved with the NOAA VDATUM software.

4. RESULTS AND DISCUSSION

4.1 Image georectification and video stabilization

Image georectification and stabilization are crucial steps for the whole workflow since a small error on the coordinates reprojection or the variation of 1^o for camera azimuth, depending on the flight height, can lead to errors greater than meters and lead to inaccurate depth estimation by the algorithm [15]. To try and achieve a good georectification result, the 5 GCP's were spread throughout the imaged area to avoid overfitting of the reprojection of image coordinates into world coordinates in certain parts and coarse reprojection in others. Projection errors fell under centimeters for both the x and y coordinates, with the greatest errors being -0.0173 m and 0.0398 m, respectively, which can be considered satisfactory according to the values reported in [16]. Although the UAS was able to keep its position with low variation, due to the incidence of wind gusts faster than 11 mph, the camera presented a standard deviation in azimuth, tilt, and roll angle of 1.3503^o, 0.0772^o, and 0.1413^o, respectively. The variation of tilt and roll angles are smaller than the ones found in [17], which were considered small enough to assume a fixed camera position. However, in this study, the camera azimuth variation was much greater than what is acceptable for assuming a stable UAS, so the 5 GCPs were used as stabilization control points for the stabilization process. After image-stabilization, the frames presented standard deviation values of 0.32 m, 0.18 m, and 0.37 m for x, y, and z, respectively. The standard deviation values for x and y are a little higher than the values considered to reflect a stable camera, but as pointed out by [17], small changes in camera orientation angles have more effect on image reprojection than the small changes in camera positioning.

4.2 Bathymetry map accuracy evaluation

The resulting depth map presented a solved area of approximately 400 m^2 with depth values ranging between 0.12 m and 3 m. With the estimated depth map, the algorithm also provides an internal quality assessment by calculating the estimated depth error map, where errors of approximately 0.6 m were located on the crest of the sandbars and spread throughout the right upper region of the area shown in Figure 2. The highest error values are present on the edges of ROI, which is caused by the boundary problem. It is needed to point out that the internal quality assessment can only be taken as qualitative information and used for detecting areas that potentially would present higher errors. cBathy error prediction method has been reported to inaccurately represent the observed measurement error relative to ground truth [16].

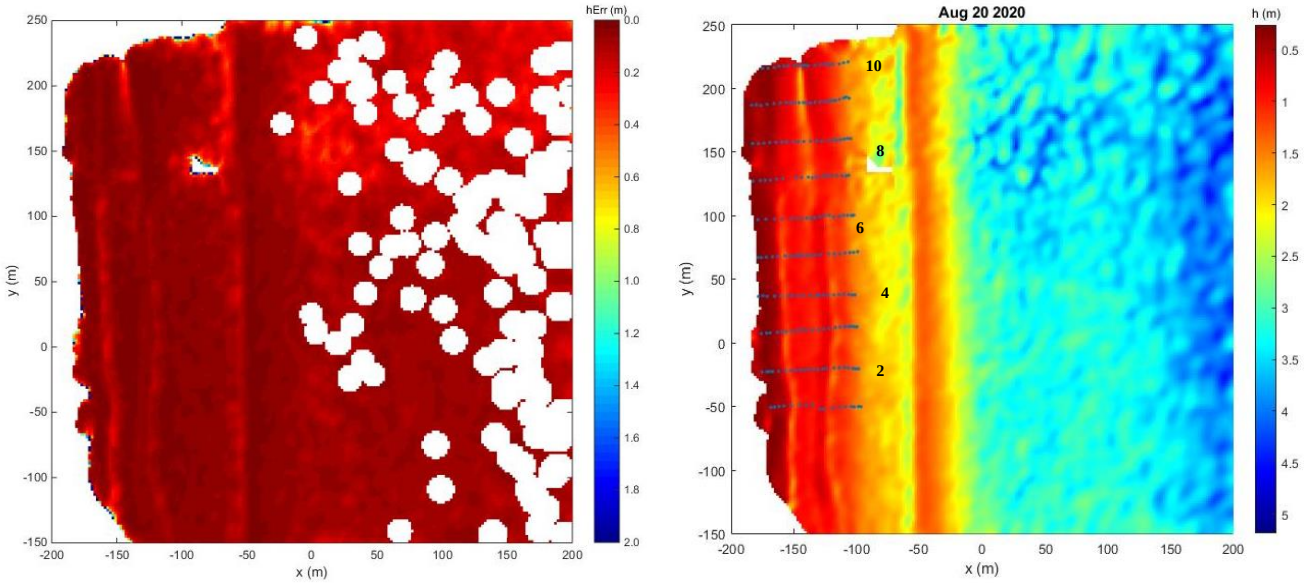

Figure 2. Left: Estimated depth error produced by cBathy internal quality assessment. Right: Resulting depth map with the surveyed transects overlayed.

The accuracy assessment results using the transect data are only related to areas with depth smaller than 2 m due to the limitations of the ground truthing methodology: transects extended until about 80 m offshore, covering only two out of the 3 existing sandbars in the area. Using the collected reference data, the root mean square error (RMSE) based on all computed differences in depth (UAS depth minus ground truth depth) was 0.21 m with a positive bias of 0.09 m. Prior work using solely the cBathy algorithm has reported depth accuracies under 0.50 m, with the lowest value reported in [18] of 0.34 m RMSE for areas with depth shallower than 5 m. Nonetheless, the observed overall RMSE value is not much greater than the general RMSE of 0.17 m obtained in a study by [19] for a beach in Virginia, USA, with similar type wave conditions using a multicamera UAS. The accuracy obtained by [19] was due to a modified workflow combining SfM photogrammetry and cBathy algorithm for the generation of a seamless topo-bathymetric map.

The accuracy assessment by transect showed a variation of RMSE between 0.13 m and 0.34 m, being the lowest and highest values, corresponding to transects 8 and 10, respectively. Transect 8 presented a low positive bias of 0.05 m, which was led mostly by the depth underestimation of the seaward side of the sandbars. Depth overestimation was observed on the trough part of the second sandbar with a difference of approximately 0.22 m as observed in Figure 3. This depth overestimation in the sandbar trough regions is observed in all transects and such phenomenon is induced by the sudden shift of the Modulation Transfer Function (MTF) due to the rapid change of image pixel values from low values, related to the wave shoaling process happening at the sandbar, to brighter values related to wave foam caused by wave breaking. So, this sudden shift of the MTF will be translated to an increase in wave speed and, consequently, an increase in depth, [17].

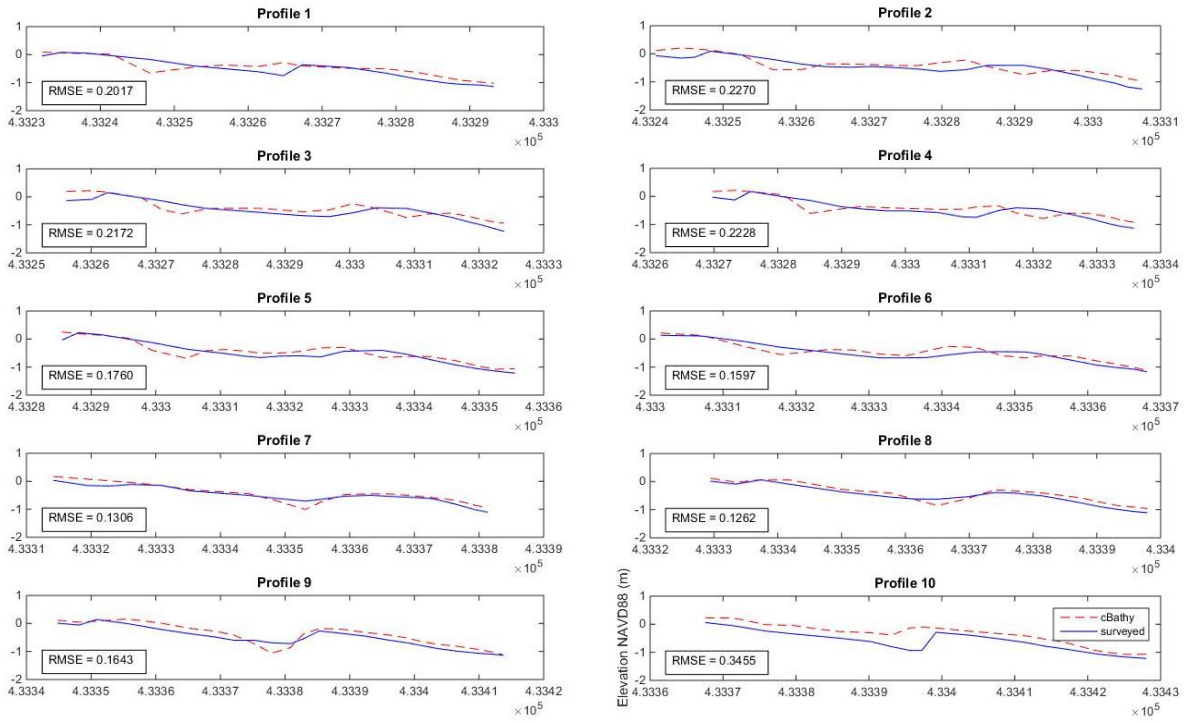

Figure 3. Cross-shore profiles of the estimated (red dashed line) and measured elevation (blue line). Elevation in orthometric height, NAVD88 vertical datum.

5. CONCLUSION

Overall, the UAS videography depth inversion algorithm using cBathy provided a reasonably good result relative to the ground truth bathymetry data. The overall RMSE of 0.21 m is very close to the 0.20 m threshold established by the International Hydrographic Organization (IHO) for bathymetric accuracy [20]. However, the method provided overestimation in the breaking zones due to the sudden shift from low pixel intensities along the wavefront to brighter values caused by the breaking wave foam. Furthermore, these results represent only one case study in relatively small amplitude wave conditions and only out to a depth of approximately 2 m for the ground truth data.

cBathy has proved to deliver good accuracy for areas with small waves in previous works, which enforce its potential to become a viable technique when implemented with small UAS for low-cost and high-resolution bathymetric mapping in coastal turbid waters. The results found in this study show that the algorithm can estimate depths with accuracy close to what is required for navigation chart updating. Notwithstanding, this conclusion needs to be taken with caution because the accuracy assessment was based on reference data that extended only 80 m seaward, and as mentioned above, to limited depths of up to 2 m. The analysis was also conducted over a relatively localized areal extent. Therefore, it is recommended that further studies covering varying surf zone conditions and with better ground truth data at deeper depths across larger alongshore areas be conducted to derive a better understanding of the technique's reliability and performance.

With some improvements, the UAS-based cBathy technique can be the solution or complementary method for localized bathymetric mapping to other techniques, for instance, Satellite-Derived Bathymetry (SDB) or SfM photo-bathymetry, especially in situations of poor visibility waters. However, before the application of this depth inversion technique or alternatives, it is necessary to take into consideration the method's inherent limitations and the environmental characteristics of the targeted study site.

6. ACKNOWLEDGMENTS

This publication was prepared by Texas A&M University-Corpus Christi using Federal funds under award NA18NOS4000198 from the National Oceanic and Atmospheric Administration, U.S. Department of Commerce. The statements, findings, conclusions, and recommendations are those of the author(s) and do not necessarily reflect the views of the National Oceanic and Atmospheric Administration or the U.S. Department of Commerce.

7. REFERENCES

[1] Neumann, B., Vafeidis, A. T., Zimmermann, J. & Nicholls, R. J., "Future Coastal Population Growth and Exposure to Sea-Level Rise and Coastal Flooding—A Global Assessment," PLOS ONE 10 (3), e0118571 (2015).

[2] Salameh, E. et al., "Monitoring beach topography and nearshore bathymetry using spaceborne remote sensing: A review,". Remote Sensing, 11(19), 2212 (2019).

[3] Klemas, V. V., The role of remote sensing in predicting and determining coastal storm impacts. Journal of Coastal Research, 25(6), 1264-1275 (2009).

[4] Jawak, S. D., Vadlamani, S. S., & Luis, A. J., "A synoptic review on deriving bathymetry information using remote sensing technologies: models, methods and comparisons," Advances in Remote Sensing 4(02), 147 (2015).

[5] Hodúl, M., Bird, S., Knudby, A., & Chénier, R., "Satellite derived photogrammetric bathymetry,". ISPRS Journal of Photogrammetry and Remote Sensing 142, 268-277 (2018).

[6] Shintani, C., & Fonstad, M. A., "Comparing remote-sensing techniques collecting bathymetric data from a gravel-bed river,". International journal of remote sensing, 38(8-10), 2883-2902(2017).

[7] Dean, R. G., & Dalrymple, R. A., [Water wave mechanics for engineers and scientists], World Scientific Publishing Company, (2), (1991).

[8] Holman, R., & Haller, M. C., "Remote sensing of the nearshore," Annual Review of Marine Science, 5, 95-113 (2013).

[9] Williams, W. W., "The determination of gradients on enemy-held beaches," The Geographical Journal, 109(1/3), 76-90(1947).

[10] Holman, R., Plant, N., & Holland, T., "cBathy: A robust algorithm for estimating nearshore bathymetry," Journal of geophysical research: Oceans, 118(5), 2595-2609 (2013).

[11] Holland, K. T., Lalejini, D. M., Spansel, S. D., & Holman, R. A., "Littoral environmental reconnaissance using tactical imagery from unmanned aircraft systems," Ocean Sensing and Monitoring II (7678), 767806(2010).

[12] Magicseaweed, "Fiss pass jetties surf report and forecast," Slate, 20 August 2020,

<https://magicseaweed. com/Fish-Pass-Jetties-Surf-Report/3948/>.(20 August,2020).

[13] Holman et al., "Coastal imaging research network,". <https://github.com/Coastal-Imaging-Research-Network> (23 August 2021).

[14] Bruder, B. L., Brodie, K. L., "CIRN Quantitative Coastal Imaging Toolbox,". SoftwareX, 12, 100582 (2020).

[15] Aarnink,J.L.,"Bathymetry mapping using drone imagery," Slate, 2 July 2017, <https://repository.tudelft.nl/islandora/object/uuid:d607109b-5891-46bc-8670-fc9b99a2b409> (23 August 2021).

[16] Vos, K., "Remote sensing of the nearshore zone using a rotary-wing UAV," Slate 8 August 2017, <https://www.researchgate.net/profile/Kilian-Vos/publication/328900961_Remote_sensing_of_the_nearshore_zone_using_a_rotary-wing_UAV/links/5bf4c2dc299bf1124fe21a15/Remote-sensing-of-the-nearshore-zone-using-a-rotary-wing-UAV.pdf> (23 August 2021)

[17] Bergsma, E. W., Almar, R., de Almeida, L. P. M., & Sall, M., "On the operational use of UAVs for video-derived bathymetry," Coastal Engineering, 152, 103527 (2019).

[18] Rutten, J., de Jong, S. M., Ruessink, G., "Accuracy of nearshore bathymetry inverted from X-band radar and optical video data," IEEE Transactions on Geoscience and Remote Sensing, 55(2), 1106-1116(2016).

[19] Brodie, K. L., Bruder, B. L., Slocum, R. K., & Spore, N. J.,"Simultaneous mapping of coastal topography and bathymetry from a lightweight multicamera UAS," IEEE Transactions on Geoscience and Remote Sensing, 57(9), 6844-6864(2019).

[20] IHO., [IHO Standards for Hydrographic Surveys], International Hydrographic Bureau, Monaco, 36(2008).